

Article

Not peer-reviewed version

---

# Establishment of a Novel Cancer-Specific Anti-HER2 Monoclonal Antibody H2Mab-250/H2CasMab-2 for Breast Cancers

---

Mika K Kaneko , [Hiroyuki Suzuki](#) <sup>\*</sup> , [Tomokazu Ohishi](#) , [Tomohiro Tanaka](#) , [Yukinari Kato](#) <sup>\*</sup>

Posted Date: 28 November 2023

doi: 10.20944/preprints202309.0906.v3

Keywords: HER2; cancer-specific monoclonal antibody; screening; epitope; flow cytometry



Preprints.org is a free multidiscipline platform providing preprint service that is dedicated to making early versions of research outputs permanently available and citable. Preprints posted at Preprints.org appear in Web of Science, Crossref, Google Scholar, Scilit, Europe PMC.

Copyright: This is an open access article distributed under the Creative Commons Attribution License which permits unrestricted use, distribution, and reproduction in any medium, provided the original work is properly cited.

Article

# Establishment of a Novel Cancer-Specific Anti-HER2 Monoclonal Antibody H<sub>2</sub>Mab-250/H<sub>2</sub>CasMab-2 for Breast Cancers

Mika K. Kaneko <sup>1,†</sup>, Hiroyuki Suzuki <sup>1,†,\*</sup>, Tomokazu Ohishi <sup>2,3</sup>, Tomohiro Tanaka <sup>1</sup> and Yukinari Kato <sup>1,\*</sup>

<sup>1</sup> Department of Antibody Drug Development, Tohoku University Graduate School of Medicine, 2-1 Seiryō-machi, Aoba-ku, Sendai, Miyagi 980-8575, Japan; mika.kaneko.d4@tohoku.ac.jp (M.K.K.); tomohiro.tanaka.b5@tohoku.ac.jp (T.T.)

<sup>2</sup> Institute of Microbial Chemistry (BIKAKEN), Numazu, Microbial Chemistry Research Foundation, 18-24 Miyamoto, Numazu-shi, Shizuoka 410-0301, Japan; ohishit@bikaken.or.jp (T.O.)

<sup>3</sup> Institute of Microbial Chemistry (BIKAKEN), Laboratory of Oncology, Microbial Chemistry Research Foundation, 3-14-23 Kamiosaki, Shinagawa-ku, Tokyo 141-0021, Japan

\* Correspondence: hiroyuki.suzuki.b4@tohoku.ac.jp (H.S.); yukinari.kato.e6@tohoku.ac.jp (Y.K.); Tel.: +81-22-717-8207 (H.S. & Y.K.)

† These authors contributed equally to this work.

**Abstract:** Overexpression of human epidermal growth factor receptor 2 (HER2) in breast and gastric cancers is an important target for monoclonal antibody (mAb) therapy. All therapeutic mAbs, including anti-HER2 mAbs, exhibit adverse effects probably due to the recognition of antigens expressed in normal cells. Therefore, tumor-selective or specific mAbs can be beneficial in reducing the adverse effects. In this study, we established a novel cancer-specific anti-HER2 antibody, named H<sub>2</sub>Mab-250/H<sub>2</sub>CasMab-2 (IgG<sub>1</sub>, kappa). H<sub>2</sub>Mab-250 reacted with HER2-positive breast cancer BT-474 and SK-BR-3 cells. Importantly, H<sub>2</sub>Mab-250 did not react with non-transformed normal epithelial cells (HaCaT and MCF 10A) and immortalized normal epithelial cells in flow cytometry. In contrast, most anti-HER2 mAbs including H<sub>2</sub>Mab-119 (IgG<sub>1</sub>, kappa) reacted with both cancer and normal epithelial cells. Furthermore, a core-fucose deleted IgG<sub>2a</sub>-type H<sub>2</sub>Mab-250 (H<sub>2</sub>Mab-250-mG<sub>2a</sub>-f) could trigger the antibody-dependent cellular cytotoxicity activity to BT-474, but not to HaCaT cells. Furthermore, H<sub>2</sub>Mab-250-mG<sub>2a</sub>-f exhibited an *in vivo* antitumor effect against BT-474 xenograft. Immunohistochemical analysis demonstrated that H<sub>2</sub>Mab-250 possesses much higher reactivity to the HER2-positive breast cancer tissues compared to H<sub>2</sub>Mab-119, and did not react with normal tissues, including heart, breast, stomach, lung, colon, kidney, and esophagus. The epitope mapping demonstrated that the Trp614 of HER2 domain IV mainly contributes to the recognition by H<sub>2</sub>Mab-250. H<sub>2</sub>Mab-250 could contribute to the development of chimeric antigen receptor-T or antibody-drug conjugates without adverse effects for breast cancer therapy.

**Keywords:** HER2; cancer-specific monoclonal antibody; screening; epitope; flow cytometry

## 1. Introduction

Human epidermal growth factor receptor 2 (HER2) is included in the receptor tyrosine kinase family of human epidermal growth factor receptors. To activate the downstream signaling, HER2 must either form heterodimers with other HER members and their specific ligands or self-assemble into ligand-independent homodimers when overexpressed [1]. The HER2 overexpression is observed in approximately 20% of breast cancers [2] and 20% of gastric cancers [3], which are associated with higher rates of recurrence, poor prognosis, and shorter overall survival. A monoclonal antibody (mAb) against HER2, trastuzumab, exhibited an anti-proliferating effect *in vitro* and a potent antitumor effect *in vivo* [4,5]. The addition of trastuzumab to chemotherapy improves objective response rates, progression-free survival, and overall survival in HER2-positive breast cancer patients with metastasis [6]. Trastuzumab has become the standard treatment for HER2-positive breast

cancers [7] and HER2-positive gastric cancers [8]. Trastuzumab has been the most effective therapy for HER2-positive breast cancer for more than 20 years [9].

The major adverse effect associated with anti-HER2 therapeutic mAbs is cardiotoxicity, thereby necessitating routine cardiac monitoring in clinics [10]. Furthermore, mice lacking *ErbB2* (ortholog of HER2) displayed embryonic lethal due to the dysfunctions associated with a lack of cardiac trabeculae [11]. Ventricular-restricted *ErbB2*-deficient mice showed the features of dilated cardiomyopathy [12]. These results indicate that HER2 is vital for normal heart development and homeostasis. Therefore, more selective anti-HER2 mAbs against tumors, which can reduce heart failures are required.

We previously established several anti-HER2 mAbs, such as H<sub>2</sub>Mab-19 (IgG<sub>2b</sub>, kappa) [13], H<sub>2</sub>Mab-41 (IgG<sub>2b</sub>, kappa) [14], H<sub>2</sub>Mab-77 (IgG<sub>1</sub>, kappa) [15], H<sub>2</sub>Mab-119 (IgG<sub>1</sub>, kappa) [16], H<sub>2</sub>Mab-139 (IgG<sub>1</sub>, kappa) [17], H<sub>2</sub>Mab-181 (IgG<sub>1</sub>, kappa) [18], H<sub>2</sub>Mab-193 (IgG<sub>1</sub>, kappa), and H<sub>2</sub>Mab-215 (IgG<sub>1</sub>, kappa) by the immunization of HER2 ectodomain (HER2ec). We further engineered the mAbs into the mouse IgG<sub>2a</sub> type (H<sub>2</sub>Mab-77-mG<sub>2a</sub>, H<sub>2</sub>Mab-119-mG<sub>2a</sub>, and H<sub>2</sub>Mab-139-mG<sub>2a</sub>, respectively), and produced the core fucose-deficient types (H<sub>2</sub>Mab-77-mG<sub>2a</sub>-f, H<sub>2</sub>Mab-119-mG<sub>2a</sub>-f, and H<sub>2</sub>Mab-139-mG<sub>2a</sub>-f, respectively) to potentiate the antibody-dependent cellular cytotoxicity (ADCC) and antitumor effect *in vivo* [19-21]. In this study, we developed and characterized a novel HER2 mAb, named H<sub>2</sub>Mab-250/H<sub>2</sub>CasMab-2.

## 2. Materials and Methods

### 2.1. Cell culture

Chinese hamster ovary (CHO)-K1, BT-474, SK-BR-3, MDA-MB-468, MCF 10A, hTERT TIGKs, HBEC3-KT, hTERT-HME1, RPTEC/TERT1, and P3X63Ag8U.1 (P3U1) were obtained from the American Type Culture Collection (ATCC, Manassas, VA). Human keratinocyte HaCaT was purchased from Cell Lines Service GmbH (Eppelheim, Germany). hTCEpi, hTEC/SVVERT24-B, and HCEC-1CT were purchased from EVERCYTE (Vienna, Austria).

The cDNA of HER2 (wild type; WT) and deletion mutants (dN218, dN342, and dN511) were cloned into the pCAG-nPA16 vector. A HER2 point mutant (W614A) and HER2 WT were cloned into the pCAG-nPA-cRAPMAP vector. CHO-K1 cells were transfected with the above-mentioned vectors using a Neon transfection system (Thermo Fisher Scientific Inc., Waltham, MA). A few days after transfection, PA tag-positive cells were sorted by the cell sorter (SH800; Sony Corp., Tokyo, Japan) using NZ-1, which was originally developed as an anti-human PDPN mAb [22]. Finally, CHO/HER2 and CHO/HER2 (dN218, dN342, and dN511) cell lines were established.

CHO-K1, CHO/HER2 (WT, deletion, and point mutants), and P3U1 were cultured in Roswell Park Memorial Institute (RPMI)-1640 medium (Nacalai Tesque, Inc., Kyoto, Japan), and BT-474, SK-BR-3, MDA-MB-468, HEK293T, and HaCaT were cultured in Dulbecco's Modified Eagle Medium (DMEM) medium (Nacalai Tesque, Inc.), supplemented with 10% heat-inactivated fetal bovine serum (FBS; Thermo Fisher Scientific Inc.), 100 units/mL of penicillin, 100 µg/mL streptomycin, and 0.25 µg/mL amphotericin B (Nacalai Tesque, Inc.). Mammary epithelial cell line, MCF 10A was cultured in Mammary Epithelial Cell Basal Medium BulletKit™ (Lonza, Basel, Switzerland) supplemented with 100 ng/mL cholera toxin (Sigma-Aldrich Corp., St. Louis, MO).

Immortalized normal epithelial cell lines were maintained, as follows; hTERT TIGKs, Dermal Cell Basal Medium and Keratinocyte Growth Kit (ATCC); HBEC3-KT, Airway Epithelial Cell Basal Medium and Bronchial Epithelial Cell Growth Kit (ATCC); hTERT-HME1, Mammary Epithelial Cell Basal Medium BulletKit™ without GA-1000 (Lonza); hTCEpi, KGMTM-2 BulletKit™ (Lonza); hTEC/SVVERT24-B, OptiPRO™ SFM and GlutaMAX™-I (Thermo Fisher Scientific Inc.); RPTEC/TERT1, DMEM/F-12 and hTERT Immortalized RPTEC Growth Kit with supplement A and B (ATCC); HCEC-1CT, DMEM / M199 (4:1, Thermo Fisher Scientific Inc.), 2 % Cosmic Calf Serum (Cytiva, Marlborough, MA), 20 ng/mL hEGF (Sigma-Aldrich Corp.), 10 µg/mL insulin (Sigma-Aldrich Corp.), 2 µg/mL apo-transferrin (Sigma-Aldrich Corp.), 5 nM sodium-selenite (Sigma-Aldrich Corp.), 1 µg/mL hydrocortisone (Sigma-Aldrich Corp.).

All cell lines were cultured at 37°C in a humidified atmosphere with 5% CO<sub>2</sub> and 95% air.

## 2.2. Development of hybridomas

Anti-HER2 mAbs, such as H<sub>2</sub>Mab-119 (IgG<sub>1</sub>, kappa) [16], H<sub>2</sub>Mab-77 (IgG<sub>1</sub>, kappa) [15], H<sub>2</sub>Mab-139 (IgG<sub>1</sub>, kappa) [17], H<sub>2</sub>Mab-193 (IgG<sub>1</sub>, kappa), H<sub>2</sub>Mab-215 (IgG<sub>1</sub>, kappa), H<sub>2</sub>Mab-19 (IgG<sub>2b</sub>, kappa) [13], H<sub>2</sub>Mab-181 (IgG<sub>1</sub>, kappa) [18], and H<sub>2</sub>Mab-41 (IgG<sub>2b</sub>, kappa) [14] were established previously. H<sub>2</sub>Mab-250 (IgG<sub>1</sub>, kappa) was established by the same strategy. Briefly, BALB/c mice were immunized with recombinant HER2ec produced by LN229 cells together with Imject Alum (Thermo Fisher Scientific, Inc.). After several additional immunizations, spleen cells were fused with P3U1 cells. The culture supernatants of hybridomas were screened using enzyme-linked immunosorbent assay (ELISA) with recombinant HER2ec and flow cytometry with cell lines.

## 2.3. Production of recombinant mAb and Fab fragments

To generate recombinant H<sub>2</sub>Mab-250 and H<sub>2</sub>Mab-119, their V<sub>H</sub> cDNAs and the C<sub>H</sub> cDNA of mouse IgG<sub>1</sub> were cloned into the pCAG-Ble vector (FUJIFILM Wako Pure Chemical Corporation, Osaka, Japan). The V<sub>L</sub> cDNAs and C<sub>L</sub> cDNA of the mouse kappa light chain were also cloned into the pCAG-Neo vector (FUJIFILM Wako Pure Chemical Corporation). The vectors were transfected into ExpiCHO-S cells using the ExpiCHO Expression System (Thermo Fisher Scientific, Inc.), and Ab-Capcher (ProteNova, Kagawa, Japan) was used to purify the recombinant H<sub>2</sub>Mab-250 and H<sub>2</sub>Mab-119.

To generate H<sub>2</sub>Mab-250-Fab and H<sub>2</sub>Mab-119-Fab, their V<sub>H</sub> cDNAs and the C<sub>H1</sub> cDNA of mouse IgG<sub>1</sub> were cloned into the pCAG-Neo vector. The V<sub>L</sub> cDNAs and C<sub>L</sub> cDNA of the mouse kappa light chain were also cloned into the pCAG-Ble vector. The vectors were transfected into ExpiCHO-S cells using the ExpiCHO Expression System, and Protein G sepharose (Cytiva) was used to purify the recombinant H<sub>2</sub>Mab-250-Fab and H<sub>2</sub>Mab-119-Fab.

To generate mouse IgG<sub>2a</sub>-type H<sub>2</sub>Mab-250 (H<sub>2</sub>Mab-250-mG<sub>2a</sub>), we cloned the V<sub>H</sub> cDNA of H<sub>2</sub>Mab-250 and the C<sub>H</sub> of mouse IgG<sub>2a</sub> into the pCAG-Ble vector. The mouse kappa light chain vector of H<sub>2</sub>Mab-250 was described above. To generate the recombinant PMab-231, we cloned heavy and light chains of PMab-231 [23] into the pCAG-Neo and pCAG-Ble vectors, respectively. To produce the defucosylated form (H<sub>2</sub>Mab-250-mG<sub>2a</sub>-f and PMab-231-f), the vectors were transfected into BINDS-09 (fucosyltransferase 8-knockout ExpiCHO-S) cells using the ExpiCHO Expression System. H<sub>2</sub>Mab-250-mG<sub>2a</sub>-f and PMab-231-f were purified using Ab-Capcher.

## 2.4. Flow cytometry

Cells were collected using 0.25% trypsin and 1 mM ethylenediamine tetraacetic acid (EDTA; Nacalai Tesque, Inc.). The cells (1 × 10<sup>5</sup> cells/sample) were treated with H<sub>2</sub>Mab-250 (10 µg/mL), H<sub>2</sub>Mab-119 (10 µg/mL), or blocking buffer [control; 0.1% bovine serum albumin (BSA) in phosphate-buffered saline (PBS)] for 30 min at 4°C. Next, the cells were treated with Alexa Fluor 488-conjugated anti-mouse IgG (1:2,000; Cell Signaling Technology, Danvers, MA) for 30 min at 4°C. The fluorescence data was collected using EC800 or SA3800 Cell Analyzer (Sony Corp), and the data were analyzed using FlowJo (BD Biosciences, Franklin Lakes, NJ).

## 2.5. ADCC reporter bioassay

The ADCC reporter bioassay was performed using an ADCC Reporter Bioassay kit (Promega Corporation, Madison, WI), according to the manufacturer's instructions. Target cells (BT-474 and HaCaT, 12,500 cells per well) were cultured in a 96-well white solid plate. H<sub>2</sub>Mab-250-mG<sub>2a</sub>-f and trastuzumab (Herceptin; Chugai Pharmaceutical Co., Ltd, Tokyo, Japan) were serially diluted and added to the target cells. Jurkat cells stably expressing the human FcγRIIIa receptor and a nuclear factor of activated T-cells (NFAT) response element driving firefly luciferase, were used as effector cells. The engineered Jurkat cells (75,000 cells in 25 µl) were then added and co-cultured with

antibody-treated target cells at 37°C for 6 h. Luminescence using the Bio-Glo Luciferase Assay System was measured using a GloMax luminometer (Promega Corporation).

### 2.6. Antitumor activities of H<sub>2</sub>Mab-250-mG<sub>2a</sub>-f in breast cancer xenografts

To examine the antitumor effect of H<sub>2</sub>Mab-250-mG<sub>2a</sub>-f, animal experiments were approved by the Institutional Committee for Experiments of the Institute of Microbial Chemistry (approval no. 2023-060). During the experimental period, we monitored mice maintained in a pathogen-free environment on 11 h light/13 h dark cycle with food and water supplied ad libitum. Mice were monitored for health and weight every one or five days. We identified body weight loss exceeding 25% and maximum tumor size exceeding 3000 mm<sup>3</sup> as humane endpoints, and terminated the experiments.

We resuspended BT-474 (5 × 10<sup>6</sup> cells) in DMEM and mixed them with BD Matrigel Matrix Growth Factor Reduced (BD Biosciences, Franklin Lakes, NJ). We injected them subcutaneously into the left flank of BALB/c nude mice (female, 5 weeks old, Jackson Laboratory Japan, Kanagawa, Japan). On day 6 post-inoculation, 100 µg of H<sub>2</sub>Mab-250-mG<sub>2a</sub>-f (n=8) or control (PMab-231-f; n = 8) in 100 µL PBS were intraperitoneally injected. On days 13 and 20, additional antibody injections were performed. The tumor volume was measured on days 6, 9, 16, 20, 22, and 27 after the inoculation of cells.

### 2.7. Immunohistochemical analysis

Formalin-fixed paraffin-embedded (FFPE) tissue of HER2-positive breast cancer was obtained from Sendai Medical Center [15]. Informed consent for sample procurement and subsequent data analyses was obtained from the patient or the patient's guardian at Sendai Medical Center. Normal tissues were purchased from BioChain Institute Inc. (Eureka Drive Newark, CA) or Cybrdi Inc. (Frederick, MD). The tissue sections were autoclaved in citrate buffer (pH 6.0; Nichirei Biosciences, Inc., Tokyo, Japan) for 20 min. The blocking was performed using SuperBlock T20 (Thermo Fisher Scientific Inc.). The sections were incubated with H<sub>2</sub>Mab-250 (1, 0.5, or 0.1 µg/mL) and H<sub>2</sub>Mab-119 (0.5 or 0.1 µg/mL), and then treated with the EnVision+ Kit for mouse (Agilent Technologies, Inc., Santa Clara, CA). The chromogenic reaction was performed using 3,3'-diaminobenzidine tetrahydrochloride (DAB; Agilent Technologies, Inc.). Counterstaining was performed using hematoxylin (FUJIFILM Wako Pure Chemical Corporation) and Leica DMD108 (Leica Microsystems GmbH, Wetzlar, Germany) was used to obtain images and examine the sections.

### 2.8. ELISA

HER2ec was immobilized on Nunc Maxisorp 96-well immunoplates (Thermo Fisher Scientific Inc.) at a concentration of 1 µg/mL for 30 min at 37°C. After washing with PBS containing 0.05% (v/v) Tween 20 (PBST; Nacalai Tesque, Inc.), wells were blocked with 1% (w/v) bovine serum albumin (BSA)-containing PBST for 30 min at 37°C. The serially diluted H<sub>2</sub>Mab-250, H<sub>2</sub>Mab-250-Fab, H<sub>2</sub>Mab-119, and H<sub>2</sub>Mab-119-Fab (0.0006–10 µg/mL) were added to each well, followed by peroxidase-conjugated anti-mouse immunoglobulins (1:3000 diluted; Agilent Technologies Inc., Santa Clara, CA, USA). Enzymatic reactions were conducted using ELISA POD Substrate TMB Kit (Nacalai Tesque, Inc.) followed by the measurement of the optical density at 655 nm, using an iMark microplate reader (Bio-Rad Laboratories, Inc., Berkeley, CA, USA). The binding isotherms were fitted into the built-in, one-site binding model in GraphPad PRISM 6 (GraphPad Software, Inc., La Jolla, CA) to calculate the dissociation constant (K<sub>D</sub>).

Synthesized peptides covering the HER2 extracellular domain IV and point mutant peptides were synthesized by Sigma-Aldrich Corp. The peptides (10 µg/mL) were immobilized on Nunc Maxisorp 96-well immunoplates (Thermo Fisher Scientific Inc.). Plate washing was performed with PBS containing 0.05% (v/v) Tween 20 (PBST; Nacalai Tesque, Inc.). After blocking with 1% (w/v) BSA in PBST, H<sub>2</sub>Mab-250 (10 µg/mL) was added to each well. Then, the wells were further incubated with peroxidase-conjugated anti-mouse immunoglobulins (1:2000 dilution; Agilent Technologies, Inc.).

Enzymatic reactions were conducted using One-Step Ultra TMB. The optical density at 655 nm was measured using an iMark microplate reader.

### 2.9. Determination of $K_D$ via surface plasmon resonance (SPR)

Measurement of  $K_D$  between H<sub>2</sub>Mab-250 and the HER2 peptides was performed using SPR. H<sub>2</sub>Mab-250 was immobilized on the sensor chip CM5 in accordance with the manufacturer's protocol by Cytiva. Immobilization of H<sub>2</sub>Mab-250 (10 µg/mL in acetate buffer (pH 4.0); Cytiva) was carried out using an amine coupling reaction. The surface of the flow cell 2 of the sensor chip CM5 was treated with 1-ethyl-3-(3-dimethylaminopropyl)-carbodiimide and N-hydroxysuccinimide (NHS), followed by the injection of H<sub>2</sub>Mab-250. The  $K_D$  between H<sub>2</sub>Mab-250 and the peptides was determined using Biacore X100 (Cytiva). The binding signals were measured using a single-cycle kinetics method. The data were analyzed by 1:1 binding kinetics using Biacore X100 evaluation software (Cytiva) to determine the association rate constant ( $k_a$ ) and dissociation rate constant ( $k_d$ ) and  $K_D$ . The affinity constant ( $K_A$ ) at equilibrium was calculated as  $1/K_D$ .

## 3. Results

### 3.1. Selection of H<sub>2</sub>Mab-250 possessing the cancer-specific HER2 recognition

We immunized mice with HER2ec produced by LN229 cells. The culture supernatants of hybridomas were screened using ELISA with HER2ec. We further screened the reactivity to HER2-positive breast cancers (BT-474 and SK-BR-3) and non-transformed normal epithelial cells including HaCaT (keratinocyte) and MCF 10A (mammary gland) using flow cytometry. One of the established hybridomas, H<sub>2</sub>Mab-250 reacted with CHO/HER2, HER2-positive BT-474, and SK-BR-3 cells, but not with triple-negative MDA-MB-468 cells. H<sub>2</sub>Mab-250 did not react with HaCaT and MCF 10A cells (Figure 1A). In contrast, H<sub>2</sub>Mab-119 showed similar reactivity to both cancer and normal epithelial cells (Figure 1A). Supplementary Figure 1 shows a titration of the binding of H<sub>2</sub>Mab-250, H<sub>2</sub>Mab-250-Fab, H<sub>2</sub>Mab-119, and H<sub>2</sub>Mab-119-Fab against CHO/HER2 cells.

We next investigated the difference in the reactivity to immortalized normal epithelial cells, including hTERT TIGKs (gingiva), HBEC3-KT (lung bronchus), hTERT-HME1 (mammary gland), hTCEpi (corneal), hTEC/SVTERT24-B (thymus), RPTEC/TERT1 (kidney proximal tubule), and HCEC-1CT (colon). H<sub>2</sub>Mab-250 did not react with those normal cells, while H<sub>2</sub>Mab-119 was reactive with all immortalized normal epithelial cells (Figure 1B), indicating that H<sub>2</sub>Mab-250 possesses cancer-specific reactivity against HER2.

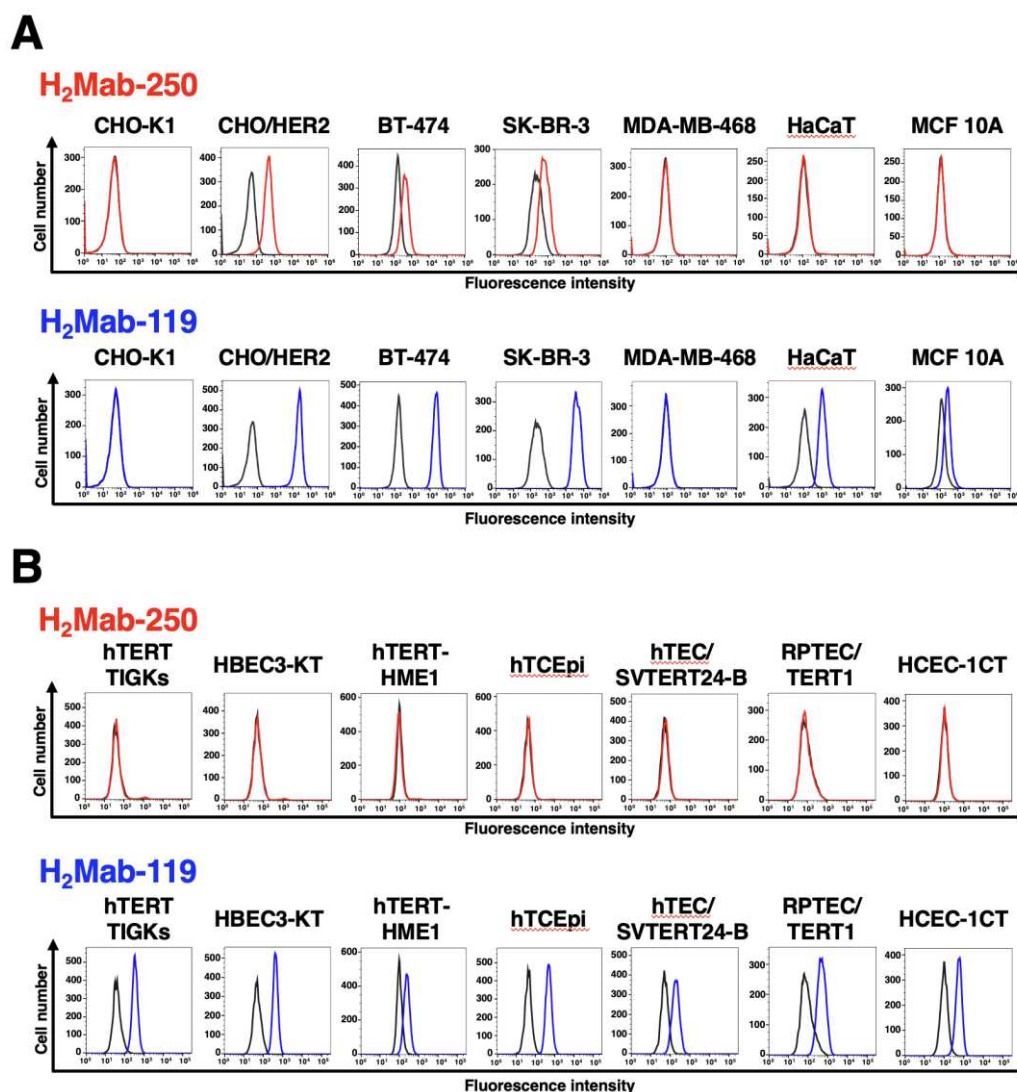


**Figure 1. Selection of H<sub>2</sub>Mab-250, a CasMab against HER2.** (A) Flow cytometry using H<sub>2</sub>Mab-250 (10  $\mu$ g/mL; Red line) and H<sub>2</sub>Mab-119 (10  $\mu$ g/mL; Blue line) against CHO-K1, CHO/HER2, HER2-positive breast cancers (BT-474 and SK-BR-3), a triple-negative breast cancer (MDA-MB-468), and non-transformed normal epithelial cells (HaCaT and MCF 10A). (B) Flow cytometry using H<sub>2</sub>Mab-250 (10  $\mu$ g/mL; Red line) and H<sub>2</sub>Mab-119 (10  $\mu$ g/mL; Blue line) against immortalized normal epithelial cells including hTERT TIGGs (gingiva), HBEC3-KT (lung bronchus), hTERT-HME1 (mammary gland), hTCEpi (corneal), hTEC/SVTERT24-B (thymus), RPTEC/TERT1 (kidney proximal tubule), and HCEC-1CT (colon). The black line represents the negative control (blocking buffer).

We next compared the reactivity of H<sub>2</sub>Mab-250 with our established anti-HER2 mAbs and trastuzumab. As shown in Figure 2, anti-HER2 domain I mAbs (H<sub>2</sub>Mab-77 [15] and H<sub>2</sub>Mab-139 [17]), anti-HER2 domain II mAbs (H<sub>2</sub>Mab-193 and H<sub>2</sub>Mab-215), anti-HER2 domain III mAbs (H<sub>2</sub>Mab-19 [13] and H<sub>2</sub>Mab-181 [18]), and anti-HER2 domain IV mAbs (H<sub>2</sub>Mab-41 [14] and trastuzumab) reacted with HER2-positive breast cancers, non-transformed normal epithelial cells, and immortalized normal epithelial cells like H<sub>2</sub>Mab-119 [16]. With some exceptions, anti-HER2 domain II mAbs (H<sub>2</sub>Mab-193 and H<sub>2</sub>Mab-215) did not react with MCF 10A and hTERT-HME1 cells. These results indicated that H<sub>2</sub>Mab-250 exhibits an exceptional reactivity compared to other anti-HER2 mAbs, including clinically approved mAb, trastuzumab.



**Figure 2. Flow cytometry using anti-HER2 mAbs.** Flow cytometry using H<sub>2</sub>Mab-77 (10 µg/mL), H<sub>2</sub>Mab-139 (10 µg/mL), H<sub>2</sub>Mab-193 (10 µg/mL), H<sub>2</sub>Mab-215 (10 µg/mL), H<sub>2</sub>Mab-19 (10 µg/mL), H<sub>2</sub>Mab-181 (10 µg/mL), H<sub>2</sub>Mab-41 (10 µg/mL), and trastuzumab (10 µg/mL) against CHO-K1, CHO/HER2, HER2-positive breast cancers (BT-474 and SK-BR-3), a triple-negative breast cancer (MDA-MB-468), non-transformed normal epithelial cells (HaCaT and MCF 10A), and immortalized normal epithelial cells, including hTERT TIGKs (gingiva), HBEC3-KT (lung bronchus), hTERT-HME1 (mammary gland), hTCEpi (corneal), hTEC/SVTERT24-B (thymus), RPTEC/TERT1 (kidney proximal tubule), and HCEC-1CT (colon). The black line represents the negative control (blocking buffer).

We next evaluated the binding affinity of H<sub>2</sub>Mab-250, H<sub>2</sub>Mab-250-Fab, H<sub>2</sub>Mab-119, and H<sub>2</sub>Mab-119-Fab to HER2ec by ELISA. As shown in Figures 3A and 3B, the  $K_D$  values of H<sub>2</sub>Mab-250 and H<sub>2</sub>Mab-250-Fab to HER2ec were determined to be  $2.6 \times 10^{-9}$  M and  $1.8 \times 10^{-8}$  M, respectively. The  $K_D$  values of H<sub>2</sub>Mab-119 and H<sub>2</sub>Mab-119-Fab to HER2ec were also determined to be  $2.6 \times 10^{-10}$  M and  $2.2 \times 10^{-9}$  M, respectively (Figures 3C and 3D). Although the binding affinity of H<sub>2</sub>Mab-250 and H<sub>2</sub>Mab-250-Fab was less than that of H<sub>2</sub>Mab-119 and H<sub>2</sub>Mab-119-Fab, respectively, H<sub>2</sub>Mab-250 and H<sub>2</sub>Mab-250-Fab exhibited high binding affinity to HER2ec.

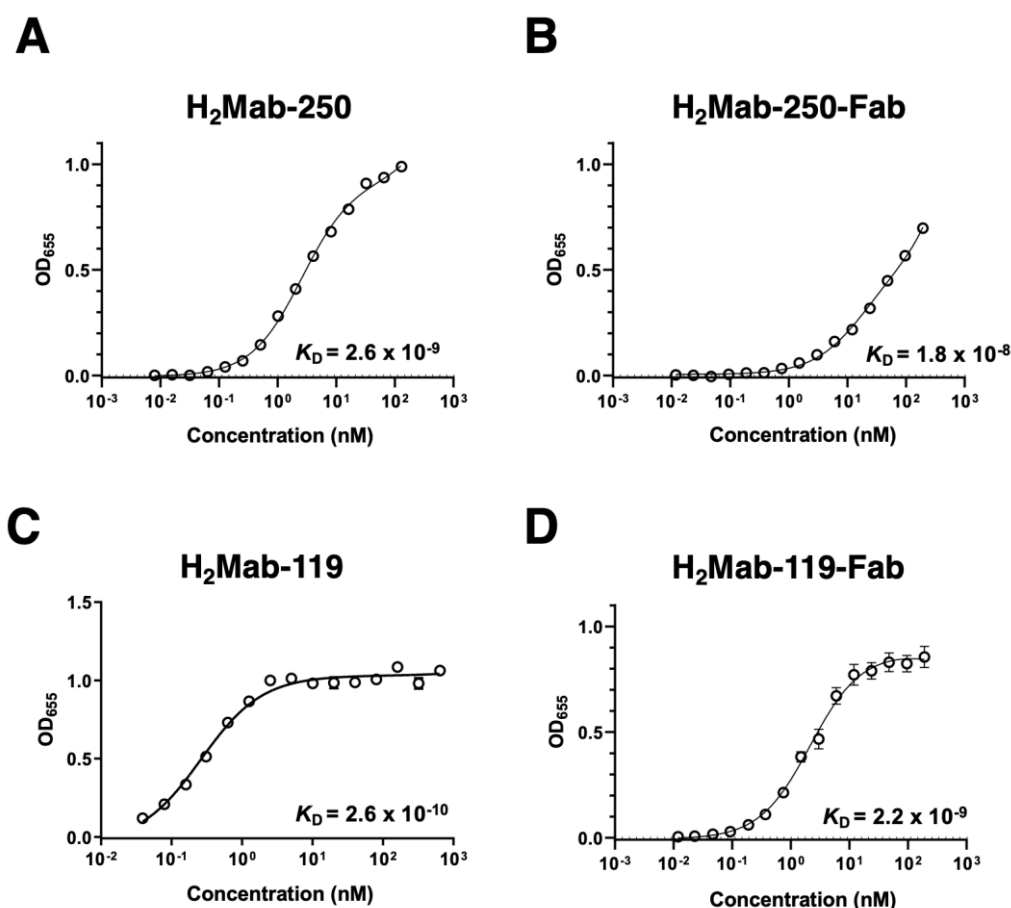


**Figure 3. Binding affinity of H<sub>2</sub>Mab-250, H<sub>2</sub>Mab-250-Fab, H<sub>2</sub>Mab-119, and H<sub>2</sub>Mab-119-Fab.** (A–D) HER2ec was immobilized on immunoplates, and then incubated with the serially diluted H<sub>2</sub>Mab-250 (A), H<sub>2</sub>Mab-250-Fab (B), H<sub>2</sub>Mab-119 (C), and H<sub>2</sub>Mab-119-Fab (D), followed by peroxidase-conjugated anti-mouse immunoglobulins. Enzymatic reactions were conducted and the optical density at 655 nm was measured. The binding isotherms were fitted into the built-in, one-site binding model in GraphPad PRISM 6 to calculate the binding affinity.

### 3.2. The ability of effector cell activation by H<sub>2</sub>Mab-250 and trastuzumab

The ADCC reporter bioassay is a bioluminescent reporter gene assay to quantify the biological activity of the antibody via FcγRIIIa-mediated pathway activation in an ADCC mechanism of action [24]. We next produced H<sub>2</sub>Mab-250-mG<sub>2a</sub>-f, the core-fucose deleted IgG<sub>2a</sub> version of H<sub>2</sub>Mab-250 using fucosyltransferase 8-deficient ExpiCHO-S (BINDS-09) cells and examined whether H<sub>2</sub>Mab-250-mG<sub>2a</sub>-f could activate ADCC program in the presence of BT-474 and HaCaT cells. To compare the ADCC pathway activation by H<sub>2</sub>Mab-250-mG<sub>2a</sub>-f and trastuzumab, we treated BT-474 and HaCaT cells with serially diluted mAbs, and then incubated with effector Jurkat cells, which express the human FcγRIIIa receptor and an NFAT response element driving firefly luciferase. As shown in Figure 4A, H<sub>2</sub>Mab-250-mG<sub>2a</sub>-f could activate the effector (EC<sub>50</sub>: 9.9 μg/mL), but it was less effective than trastuzumab (EC<sub>50</sub>: 0.053 μg/mL). Importantly, H<sub>2</sub>Mab-250-mG<sub>2a</sub>-f did not activate the effector in the presence of HaCaT cells. In contrast, trastuzumab activated the effector with similar EC<sub>50</sub> (0.036 μg/mL) to BT-474 cells (Figure 4B). These results indicated that H<sub>2</sub>Mab-250-mG<sub>2a</sub>-f selectively activates the effector cells against breast cancer cells.

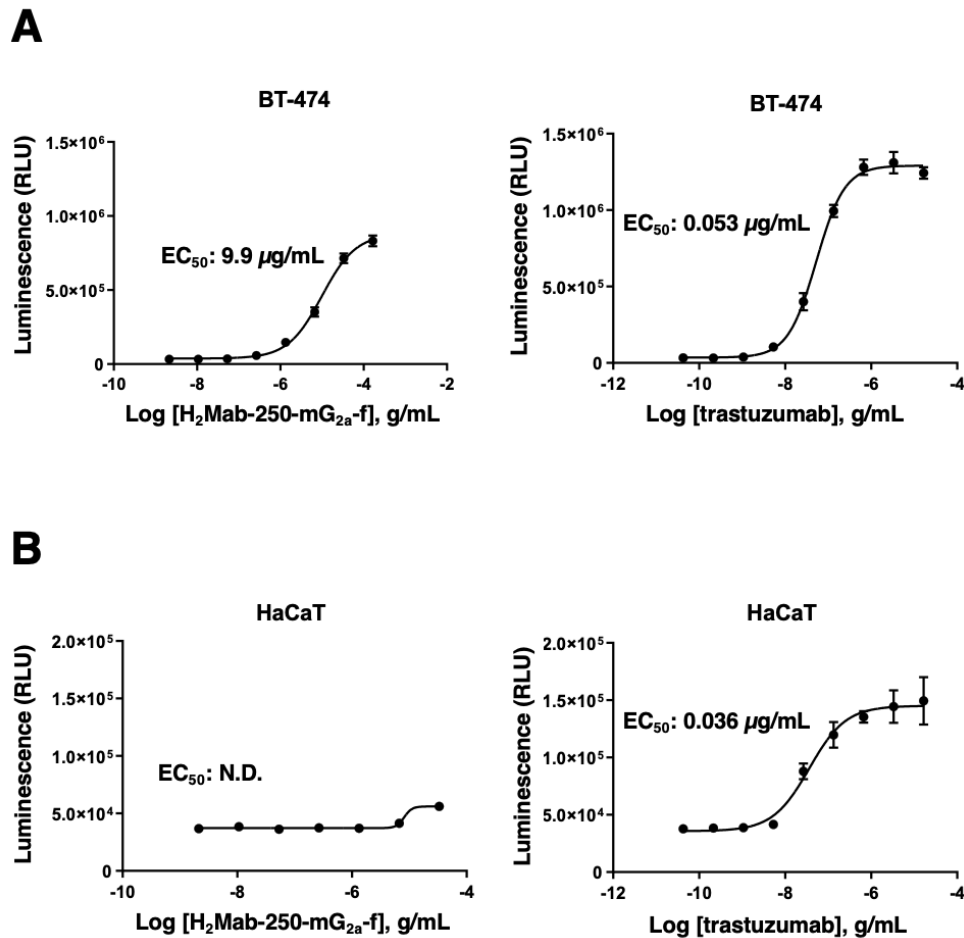


**Figure 4.** ADCC reporter assay by H<sub>2</sub>Mab-250-mG<sub>2a</sub>-f and trastuzumab in the presence of BT-474 and HaCaT cells. Target cells such as BT-474 (A) or HaCaT (B) were cultured in a 96-well white solid plate. H<sub>2</sub>Mab-250-mG<sub>2a</sub>-f and trastuzumab were serially diluted and added to the target cells. The engineered Jurkat cells were then added and co-cultured with antibody-treated target cells. Luminescence using the Bio-Glo Luciferase Assay System was measured using a GloMax luminometer. N.D., not determined. Error bars represent means  $\pm$  SDs.

### 3.3. Antitumor activities by H<sub>2</sub>Mab-250-mG<sub>2a</sub>-f

In the BT-474 xenograft models, we injected H<sub>2</sub>Mab-250-mG<sub>2a</sub>-f and a control mAb (PMab-231-f) intraperitoneally on days 6, 13, and 20 after BT-474 inoculation. We measured the tumor volume on days 6, 9, 16, 20, 22, and 27 following the inoculation. The H<sub>2</sub>Mab-250-mG<sub>2a</sub>-f administration led to a significant reduction in BT-474 xenograft on days 20 ( $P < 0.01$ ), 22 ( $P < 0.01$ ), and 27 ( $P < 0.01$ ) compared with that of the control (Figure 5A). The H<sub>2</sub>Mab-250-mG<sub>2a</sub>-f administration resulted in a 58% reduction of tumor volume compared with that of the control mAb (PMab-231-f) on day 27.

Tumors from the H<sub>2</sub>Mab-250-mG<sub>2a</sub>-f-treated mice weighed significantly less than those from the control mAb-treated mice (53% reduction;  $P < 0.01$ , Figure 5B). We resected tumors from experimental mice on day 28 are demonstrated in Figure 5C.

The body weight loss was not detected in both BT-474 xenograft-bearing mice (Figure 5D). The mice on day 27 about BT-474 xenograft were demonstrated in supplementary Figure S2.

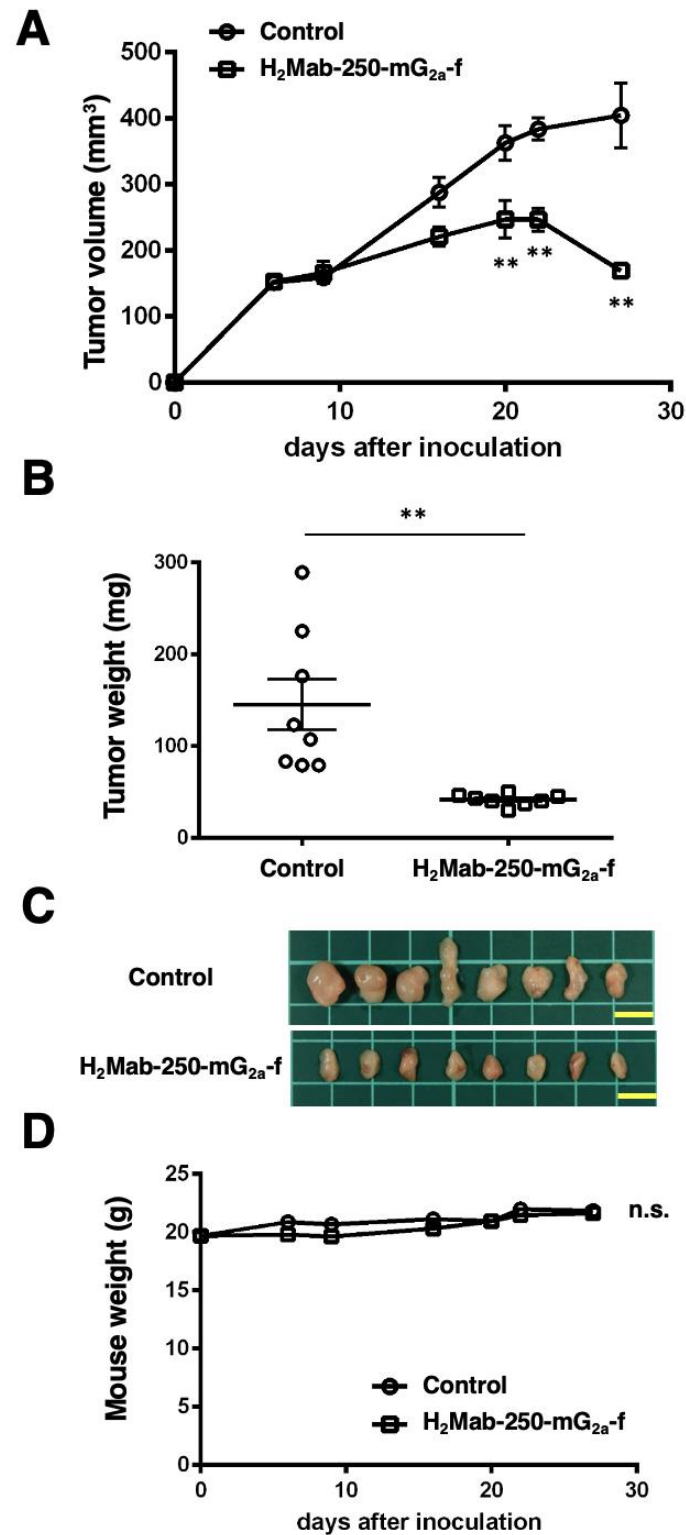


**Figure 5.** Antitumor activity of H<sub>2</sub>Mab-250-mG<sub>2a</sub>-f against BT-474 xenografts. **(A)** BT-474 cells were injected into BALB/c nude mice (day 0). On day 6, 100  $\mu$ g of H<sub>2</sub>Mab-250-mG<sub>2a</sub>-f or a control mAb (PMab-231-f) were injected into mice. On days 13 and 20, additional antibodies were injected. On days 6, 9, 16, 20, 22, and 27, the tumor volume was measured. Values are presented as the mean  $\pm$  SEM. \*\* $P < 0.01$  (ANOVA and Sidak's multiple comparisons test). **(B)** Tumor weight of BT-474 xenograft tumors on day 27. Values are presented as the mean  $\pm$  SEM. \*\* $P < 0.01$  (Two-tailed unpaired *t*-test). **(C)** The BT-474 xenograft tumors on day 27. Scale bar, 1 cm. **(D)** The body weight of BT-474 xenograft-bearing mice treated with control mAb (PMab-231-f) and H<sub>2</sub>Mab-250-mG<sub>2a</sub>-f. n.s., not significant.

### 3.4. Immunohistochemical analysis of H<sub>2</sub>Mab-250 in breast cancer and normal epithelium

Immunohistochemical analysis was performed to examine the reactivity of H<sub>2</sub>Mab-250 with normal and tumor tissue sections. In contrast to flow cytometry, H<sub>2</sub>Mab-250 exhibited more potent reactivity to the HER2-positive breast cancer section than H<sub>2</sub>Mab-119 (Figure 6A). Since all anti-HER2 therapeutic mAbs are associated with cardiotoxicity, a major adverse effect [10], the reactivity of H<sub>2</sub>Mab-250 to a normal heart was further investigated. Even with higher concentrations of H<sub>2</sub>Mab-250 (1 µg/mL), no reactivity with the normal heart could be detected (Figure 6B). Finally, the reactivity of H<sub>2</sub>Mab-250 to other normal tissues was investigated. As shown in Figure 6C, no reactivity of H<sub>2</sub>Mab-250 with any normal tissues, including breast, stomach, lung, colon, kidney, and esophagus could be observed.

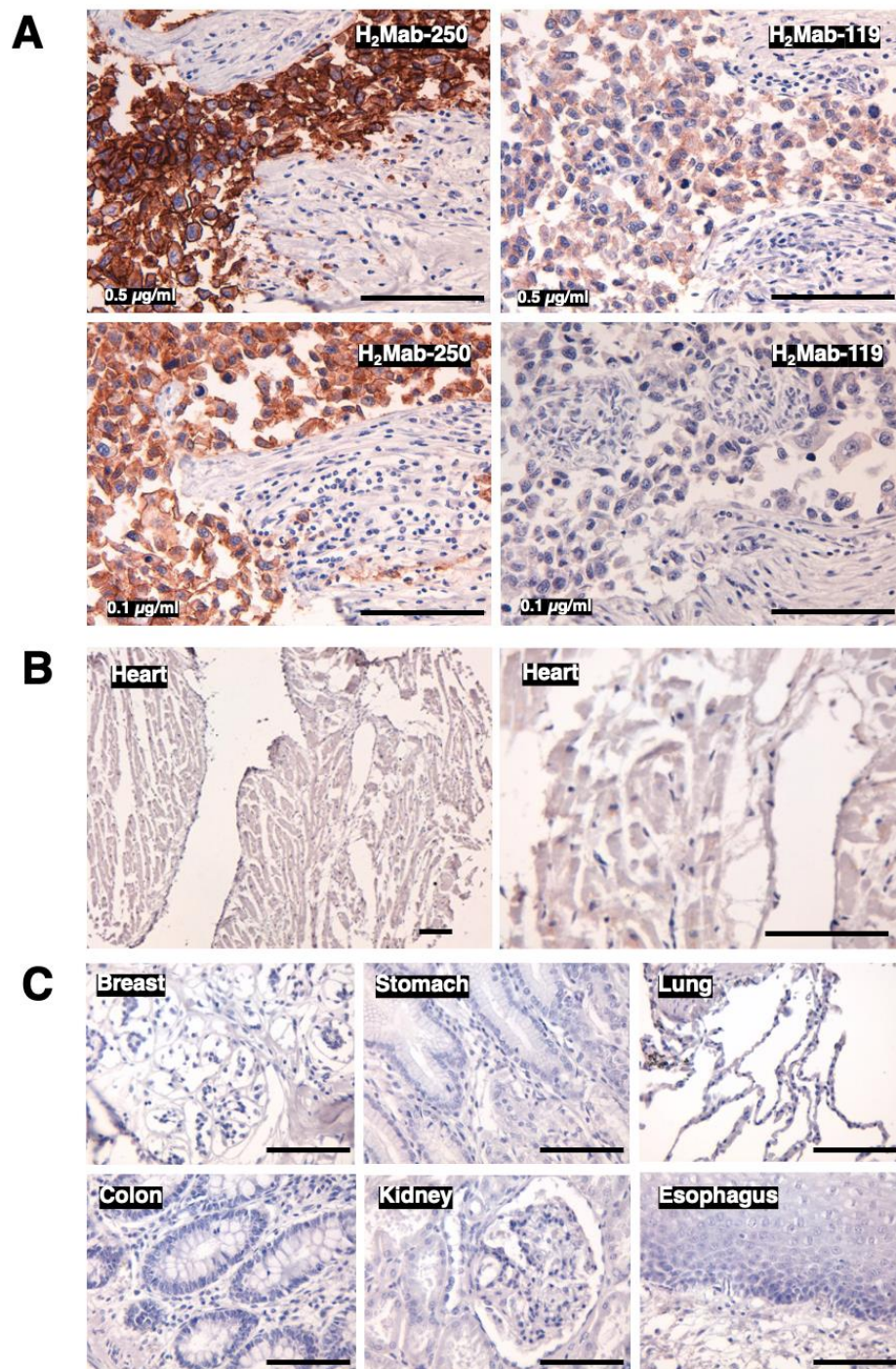


**Figure 6. Immunohistochemical analysis of H<sub>2</sub>Mab-250 in breast cancer and normal epithelium.**

(A) The HER2-positive breast cancer tissue sections were treated with H<sub>2</sub>Mab-250 or H<sub>2</sub>Mab-119 (0.1 or 0.5 µg/mL). (B) A normal heart section was treated with H<sub>2</sub>Mab-250 (1 µg/mL). (C) Sections of normal breast, stomach, lung, colon, kidney, and esophagus were treated with H<sub>2</sub>Mab-250 (0.1 µg/mL). The sections were then treated with the Envision+ kit. The chromogenic reaction was performed using DAB, and the sections were counterstained with hematoxylin. Scale bar = 100 µm.

### 3.5. Epitope identification for H<sub>2</sub>Mab-250

To determine the epitope for H<sub>2</sub>Mab-250, we examined the reactivity to CHO/HER2 (WT) and the N-terminal HER2 deletion mutants (dN218, dN342, and dN511)-expressed CHO-K1 cells (Figure 7A, left). H<sub>2</sub>Mab-250 reacted with dN218, dN342, dN511, and HER2 (WT). In contrast, H<sub>2</sub>Mab-119 reacted with only WT, but not with dN218, dN342, and dN511. Since HER2 (WT) and the deletion mutants possess PA16 tag at the N-terminus, all expression on the cell surface could be confirmed by anti-PA16 tag mAb, NZ-1 (Figure 7A, right). These results suggest that H<sub>2</sub>Mab-250 and H<sub>2</sub>Mab-119 recognize the domain IV and domain I, respectively.

For further assessment of the H<sub>2</sub>Mab-250 epitope, ELISA was performed using synthetic peptides that cover the HER2 domain IV. As shown in Figure 7B, H<sub>2</sub>Mab-250 reacted with HER2 domain IV peptide, amino acids 603–622, 613–632, but not with 593–612, 623–642, and 633–652, indicating that H<sub>2</sub>Mab-250 recognizes the 613–622 of HER2 domain IV. We further used alanine-substituted peptides of the 603–622 in HER2 domain IV. A potent reduction of the reactivity was observed in the W614A peptide (Figure 7C). We confirmed that the reactivity of H<sub>2</sub>Mab-250 completely disappeared in CHO/HER2 W614A cells in flow cytometry (Figure 7D).

The  $K_D$  of H<sub>2</sub>Mab-250 with the alanine-substituted peptides of HER2 domain IV (603–622) was measured using Biacore X100 (Table 1). The affinity constant ( $K_A$ ) at equilibrium was calculated as  $1/K_D$  (Figure 7E). Compared to the  $K_A$  of the 603–622 (WT) peptide, decreased  $K_A$  values were observed from the 613–617 region, suggesting that the 613–617 region is involved in the binding to H<sub>2</sub>Mab-250. A remarkable reduction was measured in the W614A peptide, indicating that Trp614 is mainly involved in the recognition by H<sub>2</sub>Mab-250. Supplemental Figure 3 highlights the epitope of H<sub>2</sub>Mab-250 on HER2 ectodomain structure (PDB ID: 7MN5).

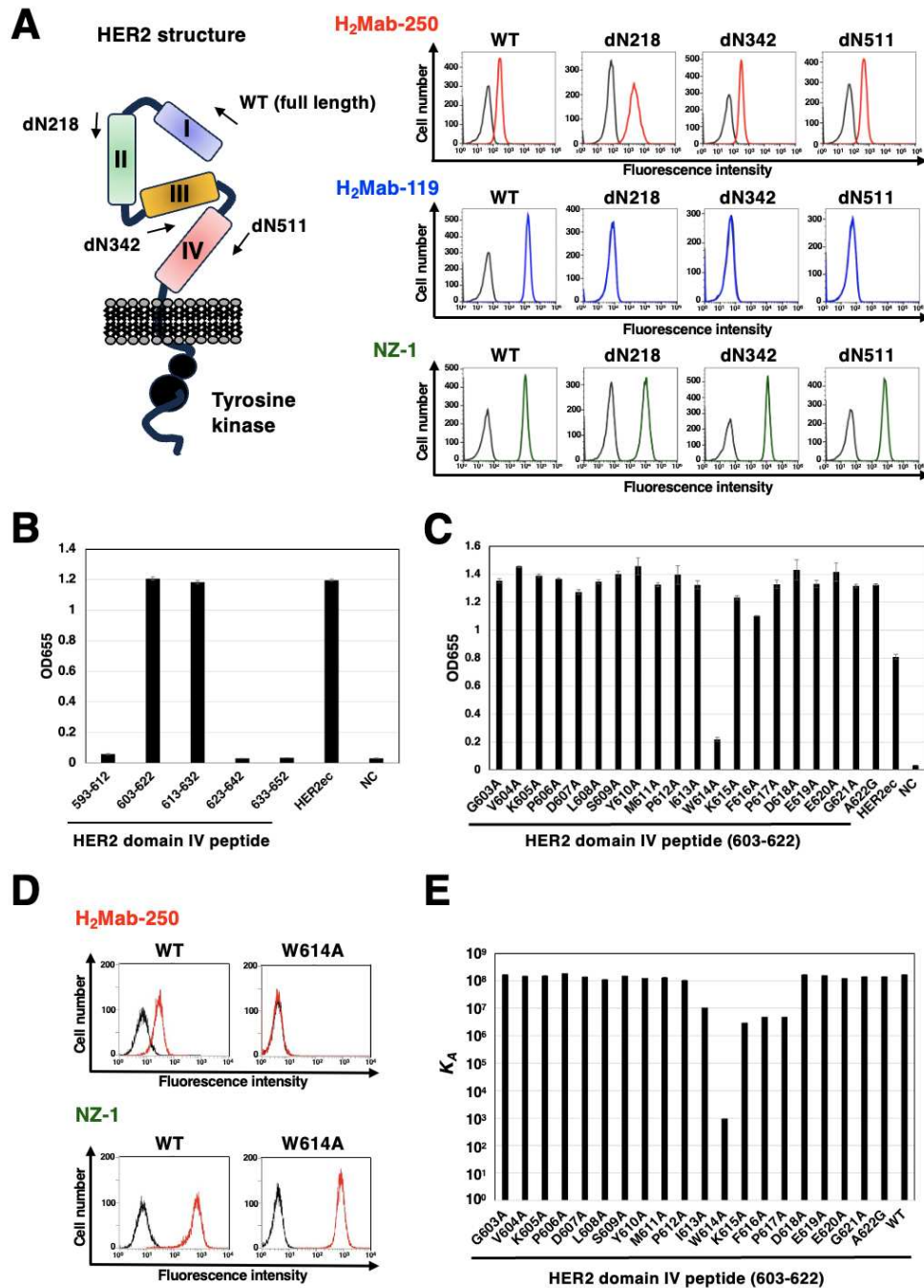


**Figure 7. Epitope identification for H<sub>2</sub>Mab-250.** (A) Epitope determination of H<sub>2</sub>Mab-250 and H<sub>2</sub>Mab-119 using flow cytometry. The schematic representation of HER2 and the deletion mutants (left). Flow cytometry using H<sub>2</sub>Mab-250 (10  $\mu$ g/mL; Red line) and H<sub>2</sub>Mab-119 (10  $\mu$ g/mL; Blue line) against CHO/HER2 (WT and deletion mutants). The cell surface expression was confirmed by an anti-PA tag mAb, NZ-1 (10  $\mu$ g/mL; Green). The black line represents the negative control (blocking buffer). (B and C) Determination of H<sub>2</sub>Mab-250 epitope by ELISA. Five synthesized peptides that cover the HER2 domain IV (B), alanine-substituted peptides of HER2 domain IV (603–622) (C), HER2ec, or buffer control (NC) were immobilized on immunoplates. The plates were incubated with H<sub>2</sub>Mab-250 (10  $\mu$ g/mL), followed by incubation with peroxidase-conjugated anti-mouse immunoglobulins. Optical density was measured at 655 nm. Error bars represent means  $\pm$  SDs. (D) Flow cytometry using H<sub>2</sub>Mab-250 (10  $\mu$ g/mL; Red line) against CHO/HER2 (WT and W614A). The cell surface expression was confirmed by an anti-PA tag mAb, NZ-1 (10  $\mu$ g/mL; Red line). The black line represents the negative control (blocking buffer). (E) Surface plasmon resonance analysis between H<sub>2</sub>Mab-250 and HER2 domain IV (603–622) peptides. The affinity constant ( $K_A$ ) at equilibrium was calculated as  $1/K_D$ .

**Table 1.** Identification of H<sub>2</sub>Mab-250 epitope using point mutants by Biacore.

Peptide	Sequence	$K_D$ (M)
603-622 (WT)	GVKPDLSYMPIWKFPDEEGA	$5.8 \times 10^{-9}$
G603A	AVKPDLSYMPIWKFPDEEGA	$5.9 \times 10^{-9}$
V604A	GAKPDLSYMPIWKFPDEEGA	$6.5 \times 10^{-9}$
K605A	GVAPDLSYMPIWKFPDEEGA	$6.5 \times 10^{-9}$
P606A	GVKADLSYMPIWKFPDEEGA	$5.3 \times 10^{-9}$
D607A	GVKPALSYMPIWKFPDEEGA	$7.1 \times 10^{-9}$
L608A	GVKPDASYMPIWKFPDEEGA	$8.8 \times 10^{-9}$
S609A	GVKPDLAYMPIWKFPDEEGA	$6.5 \times 10^{-9}$
Y610A	GVKPDLSAMPIWKFPDEEGA	$7.9 \times 10^{-9}$
M611A	GVKPDLSYAPIWKFPDEEGA	$7.5 \times 10^{-9}$
P612A	GVKPDLSYMAIWKFPDEEGA	$9.5 \times 10^{-9}$
I613A	GVKPDLSYMPAWKFPDEEGA	$9.4 \times 10^{-8}$
W614A	GVKPDLSYMPIAKFPDEEGA	$1.1 \times 10^{-3}$
K615A	GVKPDLSYMPIWAFPDEEGA	$3.4 \times 10^{-7}$
F616A	GVKPDLSYMPIWKAPDEEGA	$2.0 \times 10^{-7}$
P617A	GVKPDLSYMPIWKFADEEGA	$2.1 \times 10^{-7}$
D618A	GVKPDLSYMPIWKFPAAEEGA	$5.8 \times 10^{-9}$
E619A	GVKPDLSYMPIWKFPDAEGA	$6.3 \times 10^{-9}$
E620A	GVKPDLSYMPIWKFPDEAGA	$8.0 \times 10^{-9}$
G621A	GVKPDLSYMPIWKFPDEEAA	$6.9 \times 10^{-9}$
A622G	GVKPDLSYMPIWKFPDEEGG	$6.9 \times 10^{-9}$

#### 4. Discussion

In this study, we developed a cancer-specific mAb targeting HER2. H<sub>2</sub>Mab-250 can recognize breast cancer cells, but not normal cells in flow cytometry (Figure 1) and immunohistochemistry (Figure 6). H<sub>2</sub>Mab-250-mG<sub>2a</sub>-f could activate ADCC against breast cancer cells, but not against normal epithelial cells (Figure 4). We also identified the H<sub>2</sub>Mab-250 epitope sequence (<sup>613</sup>IWKFP<sup>-617</sup>) by SPR analysis (Figure 7). The <sup>613</sup>IWKFP<sup>-617</sup> sequence is partially included with the wider binding epitope of trastuzumab (residues 579-625) [25]. Furthermore, no reaction was observed between H<sub>2</sub>Mab-250 and CHO/HER2 W614A in flow cytometry (Figure 7), indicating that Trp614 plays a central role in recognition by H<sub>2</sub>Mab-250. Although H<sub>2</sub>Mab-250 possesses a high affinity to epitope-containing peptide (603–622) in SPR analysis, the recognition in flow cytometry using cell lines was lower than that of H<sub>2</sub>Mab-119 (Figure 1). In contrast, H<sub>2</sub>Mab-250 exhibited a higher reactivity than H<sub>2</sub>Mab-119 in the immunohistochemical analysis using breast cancer tissues (Figure 6). This discrepancy might be induced by the possibility that the epitope sequence is partially exposed in cancer cells, but not in normal cells in clinical cancer tissues. The mechanism of recognition by H<sub>2</sub>Mab-250 should be further investigated in future studies.

For the clinical treatment of metastatic breast cancer, trastuzumab is administered in patients with HER2-overexpressing tumors, which are defined by strong and complete IHC membranous staining of more than 10% of cells (IHC 3+) and/or *in situ* hybridization (ISH)-amplified. Furthermore, trastuzumab-based antibody-drug conjugates (ADCs) such as trastuzumab-deruxtecan (T-DXd) have been evaluated in various clinical trials. Based on the studies, T-DXd has been approved in not only HER2-positive breast cancers [26,27], but also HER2-mutant lung cancer [28] and HER2-low (IHC 1+ or IHC 2+ / ISH-non-amplified) advanced breast cancer [29]. A significant number of patients can benefit from T-DXd therapy since approximately half of all breast cancers are classifiable as HER2-low [30]. Meanwhile, cardiotoxicity is the most significant toxicity associated with T-DXd [31]. Further studies are essential to evaluate *in vivo* toxicities of H<sub>2</sub>Mab-250.

H<sub>2</sub>Mab-250-mG<sub>2a</sub>-f could trigger the ADCC activity to BT-474 selectively (Figure 4). Although the effect of H<sub>2</sub>Mab-250-mG<sub>2a</sub>-f is lower than that of trastuzumab, we should consider that effector Jurkat cells express human FcγRIIIa receptor. In contrast, H<sub>2</sub>Mab-250 exhibited a superior reactivity

to HER2-positive breast cancer tissue sections in immunohistochemistry (Figure 6). Since the *in vivo* efficacy of H<sub>2</sub>Mab-250-mG<sub>2a</sub>-f against BT-474 xenograft was shown in Figure 5, clinical application of H<sub>2</sub>Mab-250 is expected. Furthermore, chimeric antigen receptor (CAR)-T cell therapy against HER2 has been evaluated in clinical studies [30]. It would be worthwhile to investigate the cancer specificity of H<sub>2</sub>Mab-250 scFv and the efficacy of CAR-T against HER2-positive tumors in the future study.

## 5. Conclusions

A novel anti-HER2 antibody, H<sub>2</sub>Mab-250 exhibited cancer specificity *in vitro* and antitumor efficacy *in vivo*. In the future, H<sub>2</sub>Mab-250 could contribute to the development of CAR-T or ADCs without adverse effects for breast cancer therapy.

**Author Contributions:** M.K.K., H.S., T.O., and T.T. performed the experiments. M.K.K. and Y.K. designed the experiments. H.S. and Y.K. analyzed the data. H.S. and Y.K. wrote the manuscript. All authors have read and agreed to the published version of the manuscript.

**Funding:** This research was supported in part by Japan Agency for Medical Research and Development (AMED) under Grant Numbers: JP23ama121008 (to Y.K.), JP23am0401013 (to Y.K.), 23bm1123027h0001 (to Y.K.), JP23ck0106730 (to Y.K.), JP18am0301010 (to Y.K.), and JP21am0101078 (to Y.K.).

**Institutional Review Board Statement:** The animal experiment to examine the antitumor effect of H<sub>2</sub>Mab-250-mG<sub>2a</sub>-f was approved by the Institutional Committee for Experiments of the Institute of Microbial Chemistry (approval no. 2023-060).

**Informed Consent Statement:** Not applicable.

**Data Availability Statement:** The data presented in this study are available in the article.

**Conflicts of Interest:** The authors declare no conflict of interest.

## References

1. Yarden, Y.; Sliwkowski, M.X. Untangling the ErbB signalling network. *Nat Rev Mol Cell Biol* **2001**, *2*, 127-137, doi:10.1038/35052073.
2. Slamon, D.J.; Clark, G.M.; Wong, S.G.; Levin, W.J.; Ullrich, A.; McGuire, W.L. Human breast cancer: correlation of relapse and survival with amplification of the HER-2/neu oncogene. *Science* **1987**, *235*, 177-182, doi:10.1126/science.3798106.
3. Van Cutsem, E.; Bang, Y.J.; Feng-Yi, F.; Xu, J.M.; Lee, K.W.; Jiao, S.C.; Chong, J.L.; López-Sánchez, R.I.; Price, T.; Gladkov, O.; et al. HER2 screening data from ToGA: targeting HER2 in gastric and gastroesophageal junction cancer. *Gastric Cancer* **2015**, *18*, 476-484, doi:10.1007/s10120-014-0402-y.
4. Cho, H.S.; Mason, K.; Ramyar, K.X.; Stanley, A.M.; Gabelli, S.B.; Denney, D.W., Jr.; Leahy, D.J. Structure of the extracellular region of HER2 alone and in complex with the Herceptin Fab. *Nature* **2003**, *421*, 756-760, doi:10.1038/nature01392.
5. Tsao, L.C.; Force, J.; Hartman, Z.C. Mechanisms of Therapeutic Antitumor Monoclonal Antibodies. *Cancer Res* **2021**, *81*, 4641-4651, doi:10.1158/0008-5472.Can-21-1109.
6. Essadi, I.; Benbrahim, Z.; Kaakoua, M.; Reverdy, T.; Corbaux, P.; Freyer, G. HER2-Positive Metastatic Breast Cancer: Available Treatments and Current Developments. *Cancers (Basel)* **2023**, *15*, doi:10.3390/cancers15061738.
7. Slamon, D.J.; Leyland-Jones, B.; Shak, S.; Fuchs, H.; Paton, V.; Bajamonde, A.; Fleming, T.; Eiermann, W.; Wolter, J.; Pegram, M.; et al. Use of chemotherapy plus a monoclonal antibody against HER2 for metastatic breast cancer that overexpresses HER2. *N Engl J Med* **2001**, *344*, 783-792, doi:10.1056/nejm200103153441101.
8. Bang, Y.J.; Van Cutsem, E.; Feyereislova, A.; Chung, H.C.; Shen, L.; Sawaki, A.; Lordick, F.; Ohtsu, A.; Omuro, Y.; Satoh, T.; et al. Trastuzumab in combination with chemotherapy versus chemotherapy alone for treatment of HER2-positive advanced gastric or gastro-oesophageal junction cancer (ToGA): a phase 3, open-label, randomised controlled trial. *Lancet* **2010**, *376*, 687-697, doi:10.1016/s0140-6736(10)61121-x.
9. Maadi, H.; Soheilifar, M.H.; Choi, W.S.; Moshtaghian, A.; Wang, Z. Trastuzumab Mechanism of Action; 20 Years of Research to Unravel a Dilemma. *Cancers (Basel)* **2021**, *13*, doi:10.3390/cancers13143540.
10. Copeland-Halperin, R.S.; Liu, J.E.; Yu, A.F. Cardiotoxicity of HER2-targeted therapies. *Curr Opin Cardiol* **2019**, *34*, 451-458, doi:10.1097/hco.0000000000000637.
11. Lee, K.F.; Simon, H.; Chen, H.; Bates, B.; Hung, M.C.; Hauser, C. Requirement for neuregulin receptor erbB2 in neural and cardiac development. *Nature* **1995**, *378*, 394-398, doi:10.1038/378394a0.

12. Crone, S.A.; Zhao, Y.Y.; Fan, L.; Gu, Y.; Minamisawa, S.; Liu, Y.; Peterson, K.L.; Chen, J.; Kahn, R.; Condorelli, G.; et al. ErbB2 is essential in the prevention of dilated cardiomyopathy. *Nat Med* **2002**, *8*, 459-465, doi:10.1038/nm0502-459.
13. Takei, J.; Kaneko, M.K.; Ohishi, T.; Kawada, M.; Harada, H.; Kato, Y. H2Mab-19, an anti-human epidermal growth factor receptor 2 monoclonal antibody exerts antitumor activity in mouse oral cancer xenografts. *Exp Ther Med* **2020**, *20*, 846-853, doi:10.3892/etm.2020.8765.
14. Tateyama, N.; Asano, T.; Ohishi, T.; Takei, J.; Hosono, H.; Nanamiya, R.; Tanaka, T.; Sano, M.; Saito, M.; Kawada, M.; et al. An Anti-HER2 Monoclonal Antibody H2Mab-41 Exerts Antitumor Activities in Mouse Xenograft Model Using Dog HER2-Overexpressed Cells. *Monoclon Antib Immunodiagn Immunother* **2021**, *40*, 184-190, doi:10.1089/mab.2021.0025.
15. Itai, S.; Fujii, Y.; Kaneko, M.K.; Yamada, S.; Nakamura, T.; Yanaka, M.; Saidoh, N.; Chang, Y.W.; Handa, S.; Takahashi, M.; et al. H2Mab-77 is a Sensitive and Specific Anti-HER2 Monoclonal Antibody Against Breast Cancer. *Monoclon Antib Immunodiagn Immunother* **2017**, *36*, 143-148, doi:10.1089/mab.2017.0026.
16. Yamada, S.; Itai, S.; Nakamura, T.; Chang, Y.W.; Harada, H.; Suzuki, H.; Kaneko, M.K.; Kato, Y. Establishment of H(2)Mab-119, an Anti-Human Epidermal Growth Factor Receptor 2 Monoclonal Antibody, Against Pancreatic Cancer. *Monoclon Antib Immunodiagn Immunother* **2017**, *36*, 287-290, doi:10.1089/mab.2017.0050.
17. Kaneko, M.K.; Yamada, S.; Itai, S.; Kato, Y. Development of an Anti-HER2 Monoclonal Antibody H2Mab-139 Against Colon Cancer. *Monoclon Antib Immunodiagn Immunother* **2018**, *37*, 59-62, doi:10.1089/mab.2017.0052.
18. Takei, J.; Asano, T.; Tanaka, T.; Sano, M.; Hosono, H.; Nanamiya, R.; Tateyama, N.; Saito, M.; Suzuki, H.; Harada, H.; et al. Development of a Novel Anti-HER2 Monoclonal Antibody H(2)Mab-181 for Gastric Cancer. *Monoclon Antib Immunodiagn Immunother* **2021**, *40*, 168-176, doi:10.1089/mab.2021.0021.
19. Tanaka, T.; Suzuki, H.; Ohishi, T.; Kaneko, M.K.; Kato, Y. Antitumor activities against breast cancers by an afucosylated anti-HER2 monoclonal antibody H2Mab-77-mG2a-f. *Preprint* **2023**, doi:10.20944/preprints202307.0900.v1.
20. Arimori, T.; Mihara, E.; Suzuki, H.; Ohishi, T.; Tanaka, T.; Kaneko, M.K.; Takagi, J.; Kato, Y. Locally misfolded HER2 expressed on cancer cells is a promising target for development of cancer-specific antibodies *Cell Press Community Review* **2023**, dx.doi.org/10.2139/ssrn.4565236, doi:dx.doi.org/10.2139/ssrn.4565236.
21. Suzuki, H.; Ohishi, T.; Nanamiya, R.; Kawada, M.; Kaneko, M.K.; Kato, Y. Defucosylated Monoclonal Antibody (H2Mab-139-mG2a-f) Exerted Antitumor Activities in Mouse Xenograft Models of Breast Cancers against Human Epidermal Growth Factor Receptor 2. *Curr. Issues Mol. Biol.* **2023**, *45*, 7734-7748, doi:doi.org/10.3390/cimb45100488.
22. Kato, Y.; Kaneko, M.K.; Kuno, A.; Uchiyama, N.; Amano, K.; Chiba, Y.; Hasegawa, Y.; Hirabayashi, J.; Narimatsu, H.; Mishima, K.; et al. Inhibition of tumor cell-induced platelet aggregation using a novel anti-podoplanin antibody reacting with its platelet-aggregation-stimulating domain. *Biochem Biophys Res Commun* **2006**, *349*, 1301-1307, doi:10.1016/j.bbrc.2006.08.171.
23. Furusawa, Y.; Kaneko, M.K.; Nakamura, T.; Itai, S.; Fukui, M.; Harada, H.; Yamada, S.; Kato, Y. Establishment of a Monoclonal Antibody PMAb-231 for Tiger Podoplanin. *Monoclon Antib Immunodiagn Immunother* **2019**, *38*, 89-95, doi:10.1089/mab.2019.0003.
24. Garvin, D.; Stecha, P.; Gilden, J.; Wang, J.; Grailer, J.; Hartnett, J.; Fan, F.; Cong, M.; Cheng, Z.J. Determining ADCC Activity of Antibody-Based Therapeutic Molecules using Two Bioluminescent Reporter-Based Bioassays. *Curr Protoc* **2021**, *1*, e296, doi:10.1002/cpz1.296.
25. Diwanji, D.; Trenker, R.; Thaker, T.M.; Wang, F.; Agard, D.A.; Verba, K.A.; Jura, N. Structures of the HER2-HER3-NRG1 $\beta$  complex reveal a dynamic dimer interface. *Nature* **2021**, *600*, 339-343, doi:10.1038/s41586-021-04084-z.
26. Modi, S.; Saura, C.; Yamashita, T.; Park, Y.H.; Kim, S.B.; Tamura, K.; Andre, F.; Iwata, H.; Ito, Y.; Tsurutani, J.; et al. Trastuzumab Deruxtecan in Previously Treated HER2-Positive Breast Cancer. *N Engl J Med* **2020**, *382*, 610-621, doi:10.1056/NEJMoa1914510.
27. Shitara, K.; Bang, Y.J.; Iwasa, S.; Sugimoto, N.; Ryu, M.H.; Sakai, D.; Chung, H.C.; Kawakami, H.; Yabusaki, H.; Lee, J.; et al. Trastuzumab Deruxtecan in Previously Treated HER2-Positive Gastric Cancer. *N Engl J Med* **2020**, *382*, 2419-2430, doi:10.1056/NEJMoa2004413.
28. Li, B.T.; Smit, E.F.; Goto, Y.; Nakagawa, K.; Udagawa, H.; Mazières, J.; Nagasaka, M.; Bazhenova, L.; Saltos, A.N.; Felip, E.; et al. Trastuzumab Deruxtecan in HER2-Mutant Non-Small-Cell Lung Cancer. *N Engl J Med* **2022**, *386*, 241-251, doi:10.1056/NEJMoa2112431.
29. Modi, S.; Jacot, W.; Yamashita, T.; Sohn, J.; Vidal, M.; Tokunaga, E.; Tsurutani, J.; Ueno, N.T.; Prat, A.; Chae, Y.S.; et al. Trastuzumab Deruxtecan in Previously Treated HER2-Low Advanced Breast Cancer. *N Engl J Med* **2022**, *387*, 9-20, doi:10.1056/NEJMoa2203690.
30. Mercogliano, M.F.; Bruni, S.; Mauro, F.L.; Schillaci, R. Emerging Targeted Therapies for HER2-Positive Breast Cancer. *Cancers (Basel)* **2023**, *15*, doi:10.3390/cancers15071987.

31. Soares, L.R.; Vilbert, M.; Rosa, V.D.L.; Oliveira, J.L.; Deus, M.M.; Freitas-Junior, R. Incidence of interstitial lung disease and cardiotoxicity with trastuzumab deruxtecan in breast cancer patients: a systematic review and single-arm meta-analysis. *ESMO Open* **2023**, *8*, 101613, doi:10.1016/j.esmoop.2023.101613.

**Disclaimer/Publisher's Note:** The statements, opinions and data contained in all publications are solely those of the individual author(s) and contributor(s) and not of MDPI and/or the editor(s). MDPI and/or the editor(s) disclaim responsibility for any injury to people or property resulting from any ideas, methods, instructions or products referred to in the content.